Experimental Evaluation for the Feasibility of Test Chamber in the Open-Loop Wind Tunnel

ISMAIL[1], JOHANIS JOHN[2], ERLANDA AUGUPTA PANE[1], RAHMAN MAULANA[2], REZA ABDU RAHMAN[1], AGRI SUWANDI[1]
[1] Department of Mechanical Engineering, Faculty of Engineering
Universitas Pancasila
Srengseng Sawah, Jagakarsa 12640, DKI Jakarta
INDONESIA
[2] Student of Mechanical Engineering, Faculty of Engineering
Universitas Pancasila
Srengseng Sawah, Jagakarsa 12640, DKI Jakarta
INDONESIA

Abstract: - The test chamber in an open-loop wind tunnel is a critical part for aerodynamic experiment. The study aims to assess the feasibility of the new design of test chamber for open–loop wind tunnel by studying the fluid characteristic and the average pressure in the test chamber. The study is done by a series experimental test for the test chamber. From experimental test, the downstream velocity in the test chamber is increased from 8.9 m/s to 12.72 m/s where the pressure gradient is ranging from 6.19 to 8.398 atm with the overall turbulence intensity for the test chamber is 0.749%. According to the results, the designed open-loop wind tunnel is acceptable to use for an aerodynamic test.

Key-Words: - test chamber, open-loop, wind tunnel, turbulence, intensity, turbulence model

Received: October 22, 2020. Revised: May 14, 2021. Accepted: May 22, 2021 Published: May 31, 2021.

1 Introduction

There is limited publication that discusses the test chamber in wind tunnel. The main reasons are due to statical symmetry of the test chamber, simple design either using a circular, square or rectangular cross section and also related with the fluid flow to the test chamber which already set from the contraction chamber [1]. In relation with the article in aerodynamic test, study of turbulence, or wind engineering, it shows the wind tunnel plays an important role to provide data to analyze the interaction between the sample and fluid flow.

Manan et.al tested a hybrid car model while Clarke et.al. testing autonomous vehicles for aerodynamic characteristics as part of the design phase [2], [3]. Other relevant studies are given in testing the hydraulic transport of particles [4], as well as in studying the interaction of magnetic fields on electrical conductivity, such as liquid metals (Mercury, Gallium, Sodium, etc.), which are influenced by the Hall effect and the entropy properties of matter due to heat that arises [4].

In most wind tunnel designs, the focus in wind tunnel construction is how to design the contraction space optimally, and this has been given in many writings such as given by Watmuff, Morel, etc. [5]–[8]. The main result expected from the construction of a wind tunnel, especially in the test room, is the creation of a uniform airflow in the wind tunnel, so that the wind tunnel is said to be appropriateness and readiness for use. Owen defines the measures that affect the quality of air flow in this tool into 4 factors, namely fluid flow uniformities, swirl, low frequency unsteadiness, and turbulence [9], while Moonen divides them into two categories, namely spatial uniformity and temporal steadiness of velocity and pressure [10].

The wind tunnel measurement quality is determined by the characteristic of the airflow and its dimension. Good if it should be supported in parallel direction and the movement of the fluid energy. The airflow uniformity inside the test chamber could be found from the wind direction and speed without neglecting entropy mode disturbance, geometry imperfections, and surface irregularities, and other factors. The parallel fluid transfer shows the uniformity of flow in the tunnel and determines the existing turbulent flow at the same time [11].

Vorticity mode disturbances, in general, are an irregular and unpredictable fluctuation of momentum related to the flow. The transfer of energy characterizes vorticity; even the movements are time-dependent. It began to emerge from the beginning since the energy entering the settling chamber [12]. Therefore, the turbulent flow at one point is a correlation of the instantaneous velocity at the three-speed components, which are u', v', and w'. The relation between these three components with the fluid flow layer tension can be written as [13] (Eq. 1 and Eq. 2):

$$\tau_{xy} = -\rho\overline{u'v'} \quad (1)$$

$$\tau_{xz} = -\rho\overline{u'w'} \quad (2)$$

Where τ is the tension of each fluid layer, ρ is the fluid density, and the bar shows the average flow resultants.

The chaotic and unpredictable movements of the fluid in the channel become the subject of investigation, and there were many studies have revealed the turbulent management methods, including when the flow enters the wind tunnel. An example of the turbulent manipulation is by adjusting the contraction space ratio from 6 to 9 [14], modify the shape and the dimensions of the honeycomb cell and place it in an optimal position, adding screen, combine honeycomb with the screen, also increasing the honeycomb hydraulic diameter as an element that influencing turbulent effect on fluids [15]–[17].

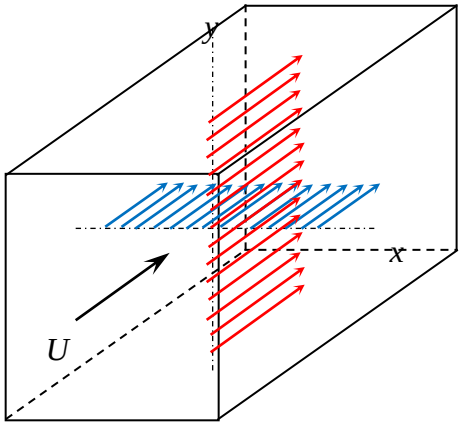

Fig. 1: Schematic diagram of the measurement point in the wind tunnel

An open-loop subsonic wind tunnel was designed and built for the aerodynamic test in this research. This type was chosen due to its size that can be easily adapted to the space of the Pancasila University Mechanical Engineering Laboratory (Fig. 2) and the ease of placement of the other laboratory instruments [7], [18]. The simulation by using Computational Fluid Dynamic (CFD) has done earlier as the preliminary design process [19]. The operational cost is also considered in constructing the open-circuit wind tunnels without neglecting its ability to provide the quality of data measurement, especially for the aerodynamic testing. The wind tunnel was designed by the focus on determining the size and geometry of the required test chamber [20]–[22], although in other studies, the initial stage of the wind tunnel design begins with determining the dimensions of the contraction space or contraction space ratio [8], [21], [23]. The wind tunnel contraction chamber in this research was designed by using the Logarithmic Derivative Profile (LDP) method or the Boerger model [7].

Fig. 2: The wind tunnel in Mechanical Engineering Laboratory

The main motivation of our study is to evaluate the feasibility of a specially designed wind tunnel. The test chamber design has many advantages such as convenience in placing the test object, larger test area, and low turbulence intensity through simulation tests with an acceptable level of wind speed uniformity [20]. Feasibility testing is an important indicator for the wind tunnel so that a feasibility test through the experiment must be carried out [24]. It is hoped that the results of the feasibility test can be used as an ideal indicator of the wind turbine design we have developed.

2 Experimental Setup

The experimental testing was conducted at the Mechanical Engineering Laboratory of Pancasila University. The test focus on the wind tunnel that has been built with its type and geometry follows the predetermined design [20]. The cross-section is the z-axis (length), x-axis (width) and y-axis (height). The test chamber sizes 750 x 750 x 1,200 mm; while the diffuser has a length of 1356 mm, the inlet nozzle has a diameter of 750 mm, and the output nozzle forms a round exit to fit the blower. The contraction chamber is square-formed with 250 mm fillet size and a 750 mm cross-section geometry size, input 1,250 mm, length 900 mm. The

contraction and diffuser chamber are made of steel, but the test chamber is made of acrylic with a thickness of 3 mm. The 5.5 kW motor becomes the axial fan drive that is placed after the diffuser. The axial fan rotating motion is the source of air drive in the wind tunnel, with six blades and 1,225 m in diameter. The axial fan draws a certain amount of air that can be regulated by using a frequency converter. The fan maximum rotational speed is 2,900 rpm. By those capabilities, the suction blower has the power to drive airflow into the tunnel with the 7.635 m^3/s average flow rate.

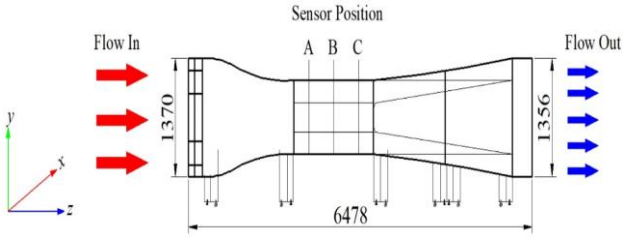

Fig. 3: Schematic diagram of the measurement point in the wind tunnel

Fig. 3 shows the schematic of the experimental arrangement. The location for determining the measurement point refers to a generally developed protocol for wind tunnel design [24], [25]. Measurement parameters that are important indicators include the mean wind speed profiles and the turbulence intensity profile. To obtain this value, the placement of the measurement points needs to be done in a specific manner.

The hot-wire anemometry sensor is placed in the test chamber, where the test chamber is divided into three cross-section parts, namely A, B, and C sections (Fig. 4). The space between each cross-section measured from the input nozzle of the test chamber where the A cross-section is 200 mm after entering the test section, the B cross-section is 600 mm from the test section and the C cross-section within 200 mm from the output nozzle of the test chamber (Fig. 4.a). At each cross-section, A, B, and C are given the test points, namely P_1, P_2, P_3, P_4, P_5, P_6, P_7, P_8, and P_9, where the length between each point is 280 mm and the closest point to the test chamber wall is 92 mm (Fig 4.b).

The measurement with hot wire anemometry is conducted at each measurement point under standard technique measurement. The data collection is taken ten times for each cross-section and yielded 90 data. The measurements on the test section are performed on the three cross-sections, the entrance area (denoted as A), the midpoint area (denoted as B), and when leaving the test section (denoted as C). There are 9 points of free stream velocity data gathering (Fig. 4.b), and velocity acquisition at each position of each cross-section is made every 10 seconds for 1 minute. After obtaining data for each point, the average position wind speed (A), (B), and (C) are also determined. Fan speeds are adjusted to produce wind speeds in the test chamber at 8 m/s, 10 m/s, and 12 m/s.

2.1 The calibration of hot-wire anemometry

The hot-wire anemometry of the U-shaped pitot-static tube is calibrated by interpolating the results of both measurements to ensure the measurement value on the hot-wire is constant. The constant voltage anemometry model is used in this experiment. The constant voltage anemometry type is used to overcome the influence of electromagnetic radiation from laboratory

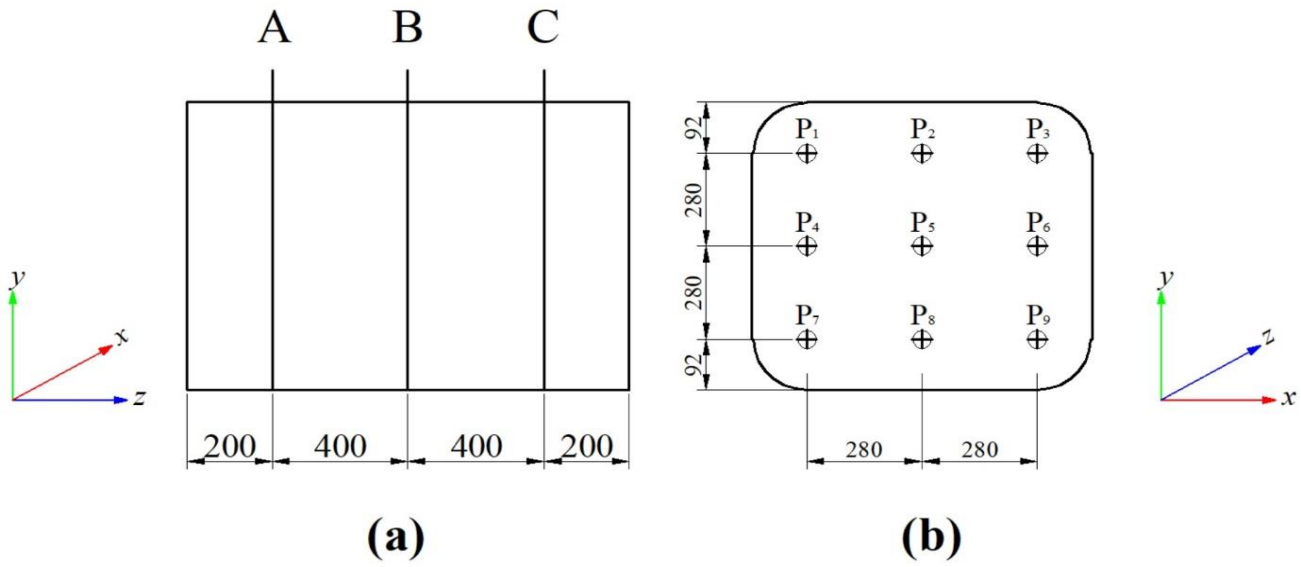

Fig. 4: (a) Cross section of sensor position at the test point (b) Hot-wire anemometry position

equipment. The hot-wire anemometry and pitot-static tubes are placed at predetermined measurement points in the wind tunnel test chamber alternately. The results of the reading of these two tools are interpolated in a velocity curve against the space. The measurement was applied ten times at P_1, P_3, P_5, P_7, and P_9. This measurement is also calibrated in all three sections (A, B, and C). The wind velocity reference is 1 m/s. The velocity value of the pitot-static tube is determined by the difference in pressure that appears on the nozzle. The pressure difference will be converted to velocity with $\Delta P = \frac{1}{2}\rho U^2$, where $\Delta P = P_{nozzle} - P_{atm}$; P is pressure in atm, U is the freestream velocity of the fluid in m/s, where the air pressure P_{atm} is 101,325 Pa.

2.2 Honeycomb and screen

The combination of honeycomb and the screen in the contraction chamber is intended to prevent the enlargement of the air velocity to the sideways lateral velocity. The magnitude of sideways flow velocity is related to the non-uniformities of the mean flow and persists for the significant downstream distance, and it contributes to the formation of turbulence in the flow following terms $\overline{uv}\,{}^{\partial U}/_{\partial y}$ of the turbulence energy equation. The honeycomb of the cells has made from metal pipes with length (l) 1,200 mm, hydraulic diameter (D_H) is 100 mm, and pipe thickness (δ) is 0.5 mm. The displacement thickness of the boundary layer inside the cell can be determined by S_g =1 - (F_1/F_0) = 0.015, with F_0 is the total area of the contraction chamber channel in which the honeycomb is mounted, and F_l is the area of the cross-section covered by the honeycomb. Two layers of the screen (stainless with mesh 7/16 in.) are placed after the honeycomb. The first screen is placed 10 cm after the honeycomb and separated 5 cm with the next screen.

3 Result and Discussion

In this experiment, the measured freestream is the velocity in the direction of the mean flow. The mean direction of flow in this experiment is parallel with the z-axis or parallel in line with the tunnel length (Fig. 3 & Fig. 4). The air velocity varies in each field and each test station, and its value is taken at the predetermined test point. The turbulence intensity is determined by Eq. 3 as the square root of the average velocity at the average downstream, where the velocity component with the perpendicular gradient to the average flows. The fluctuation velocity u' is obtained from the difference spontaneous velocity of the fluid with the average velocity is $\bar{u}$.

$$\mathrm{TI} = \frac{\sqrt{\overline{u'^2}}}{\bar{u}} .100\% \qquad (3)$$

The test velocity in the chamber is 8 m/s, 10 m/s, and 12 m/s. The Bernoulli method calculation is needed to get the preliminary velocity to come into the wind tunnel. From the calculation, the values are around 4 m/s, 5 m/s, and 6 m/s. The probing results show the average stream in the test chamber is 8.9 m/s from the velocity of 4 m/s, 10.91 m/s from 5 m/s, and finally for 6 m/s is obtained 12.72 m/s.

Fig. 5 shows the comparison between the experimental data and simulation results from previous research [19] at the test point with various reference velocities are 4 m/s, 5 m/s, and 6 m/s. even though the airstream velocity in the experiment shows a lower value than the CFD simulation value. Their velocity gradient curve has a same trend are ranging from 0.067 to 0.1, except for $\bar{u}$ = 5 m/s, both have a same curve gradient which is 0.067. At specific points, the two downstream closed to each other like P_2 and P_8 with 4 m/s, then P_5 and P_7 at 5 m/s. At a velocity test of 4 m/s, the difference in the average airflow in the test chamber between the results of the experiment with the simulation is equal to 0.43 m/s, 5 m/s produced an average velocity of 0.38 m/s, while at 6 m/s is obtained the difference between the experimental results of the simulation of 0.57 m/s. Thus, the average difference between the results of the simulations with experiments is 0.45 m/s.

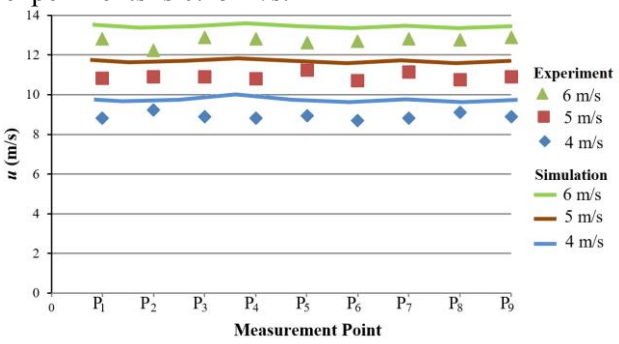

Fig. 4: The comparison of the air flow velocity in experiment and simulation from [19]

The turbulent intensity from experiment test at the measurement points show similar gradients with the simulation result, though the result from simulation is slightly lower than the experimental results (Fig. 6) where the turbulence intensity that obtained from experiments are 0.693%, 0.944% and 0.609% at various mean velocities are 8.9 m/s, 10.91 m/s and 12.72 m/s, respectively. The turbulence intensity level increases when the airflow passes through

section B (Fig. 4a) but decreases when it crosses section C (Fig. 4a). This condition is also given to simulation data. It needs to consider that during the experiment, there is a hot-wire anemometry in the test chamber, which may affect the turbulence fluctuations. Besides, the value of turbulence intensity at point P_5 decreases compared to the other points, especially from the numerical results that consistently down. It is due to P_5 is the centerline point of crosswise A, B, and C.

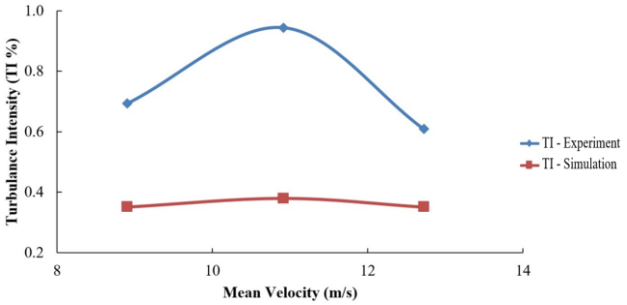

Fig. 6: The average of Turbulence Intensity (TI)

Fig. 7 shows the correlation between the pressure in the test chamber and turbulence intensity. Several relevant studies are summarized in Table 1 and help make a better conclusion regarding the experiment results. Youngjin Seo et al. [16] conclude that an increase in mean velocities would be proportional to the intensity of turbulence. Maria et al. [7] find the turbulence intensity tends to be constant even though the freestream velocity increase. The experimental test in this study shows different results where the turbulence intensity varies with the mean velocity and tends to decreases when the downstream rises.

Tabel 1. The comparison of turbulent intensity from various research

$\bar{u}$ (m/s)	**Turbulence Intensity average** (%)			
	Seo, Y., et al. [16]	Maria et al.[7]	Ghorbanian [26]	Ismail et.al.
1.4	2.557			
1.8	3.732			
2.7	4.639			
8.9		0.69*		0.693
10.91				0.944
12.72				0.609
80.00			0.302	

* The average turbulent intensity for all-speed

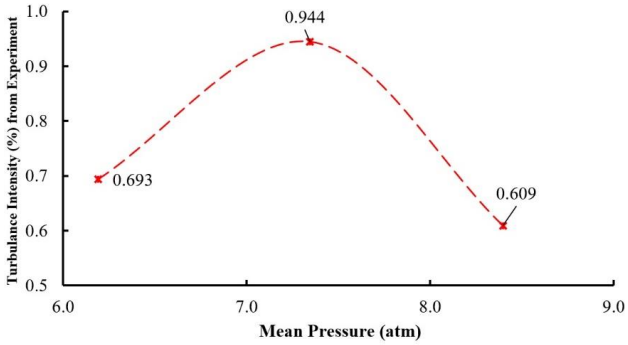

Fig. 7: The relation between turbulence intensity and mean pressure

Maria et. al. and Ghorbanian gave the average turbulence intensity value measured in the wind tunnel contraction chamber, in which Youngjin Seo et. al. displays all turbulence intensities at each flow velocity reference in the wind tunnel contraction space. As a comparison, the value of turbulence intensity by Maria as the average value is 0.69, whereas if the turbulence intensity by Ismail et.al. You will get the average value is 0.75, and if wepay attention to the average turbulence intensity value from Younjin Seo et.al. then the average result will be 3.64. The Ghorbanian gives a turbulence intensity value of 0.302 at a reference speed of 80 m/s.

Although the turbulence intensity values from several studies above are obtained from measurements in different parts of the wind tunnel, by reviewing the value of the contraction ratio of the four studies above, namely Ghorbanian, it gives a contraction ratio C_R = 7, the C_R Maria et.al. are ranging from 6.25 - 9.5. Then for C_R Youngjin Seo et.al. is 10, while Ismail et.al. is 2.4. The ideal contraction space ratio values as given by James H. Bell and Mehta are in the range 6 - 12 [1].

The three previous articles provide that the C_R value is within the range required in general, while the C_R from Ismail et.al. is below the tolerance interval it should be. This case can be understood by reviewing the different approach given by Ismail et.al., where Ismail et.al. focuses on the design and construction of the test room first, the other space adjusts later [20]. This method results in limited other spatial dimensions and the ratio of the space for contraction to be outside the required space ratio range. However, these conditions can still provide a value for the intensity of turbulence in a proper test space.

4 Conclusion

A series of experimental studies were carried out to evaluate the feasibility of the overall test chamber of

a subsonic open-loop wind tunnel, and the results were compared with previous studies of relevant researches. This study has provided another alternative in designing and constructing wind tunnels due to limited space, namely in the form of a way to design and manufacture parts of the test space first, then the other dimensions of the room are adjusted to the rest of the room.

The results of the experimental data show that the average level of turbulence intensity in the subsonic wind tunnel test chamber is 0.749%, which considerably feasible to be used for the aerodynamic test. Regardless of the geometry of the test chamber and its surface character, the various mean reference velocities in the test chamber provide the stability of the current and prove that the airflow typical inside the test chamber of tunnel is uniform.

References:

[1] J. H. Bell and R. D. Mehta, "Contraction Design For Small Low-Speed Wind Tunnels," Department of Aeronautics and Astronautics, Stanford University, California US, 1988.

[2] M. Desai, S. A. Channiwala, and H. J. Nagarsheth, "Experimental and Computational Aerodynamic Investigations of a Car 2 Experimental Approach," *WSEAS Trans. FLUID Mech.*, vol. 3, no. 4, pp. 359–368, 2008.

[3] D. B. Clarke, P. A. Brandner, and G. J. Walker, "Experimental and Computational Investigation of Flow Around a 3-1 Prolate Spheroid," *WSEAS Trans. FLUID Mech.*, vol. 3, no. 3, pp. 207–217, 2008.

[4] A. A. Opanuga, O. O. Agboola, H. I. Okagbue, and A. M. Olanrewaju, "Entropy generation of MHD poiseuille flow with hall and joule heating effects," *Int. J. Mech.*, vol. 14, pp. 28–36, 2020.

[5] T. Morel, "Comprehensive Design of Axisymmetric Wind Tunnel Contractions," *J. Fluids Eng.*, pp. 1–9, 1975.

[6] J. H. Watmuff, "Wind Tunnel Contraction Design," in *9th Australasian Fluid Mechanics Conference*, 1986, pp. 472–475.

[7] M. Rodríguez Lastra *et al.*, "Novel design and experimental validation of a contraction nozzle for aerodynamic measurements in a subsonic wind tunnel," *J. Wind Eng. Ind. Aerodyn.*, vol. 118, pp. 35–43, 2013.

[8] E. S. Zanoun, "Flow characteristics in low-speed wind tunnel contractions: Simulation and testing," *Alexandria Eng. J.*, vol. 57, no. 4, pp. 2265–2277, 2017.

[9] F. K. Owen and A. K. Owen, "Measurement and assessment of wind tunnel flow quality," *Prog. Aerosp. Sci.*, vol. 44, pp. 315–348, 2008.

[10] P. Moonen, B. Blocken, and J. Carmeliet, "Indicators for the evaluation of wind tunnel test section flow quality and application to a numerical closed-circuit wind tunnel," *J. Wind Eng. Ind. Aerodyn.*, vol. 95, no. 9–11, pp. 1289–1314, 2007.

[11] W. Zhang, L. L. Chen, X. Y. Guo, and L. Sun, "Nonlinear dynamical behaviors of deploying wings in subsonic air flow," *J. Fluids Struct.*, vol. 74, pp. 340–355, 2017.

[12] R. Feil, M. Hajek, and J. Rauleder, "Vibratory load predictions of a high-advance-ratio coaxial rotor system validated by wind tunnel tests," *J. Fluids Struct.*, vol. 92, p. 102764, 2020.

[13] C. D. Argyropoulos and N. C. Markatos, "Recent advances on the numerical modelling of turbulent flows," *Appl. Math. Model.*, vol. 39, no. 2, pp. 693–732, 2015.

[14] D. Golubić, W. Meile, G. Brenn, and H. Kozmar, "Wind-tunnel analysis of natural ventilation in a generic building in sheltered and unsheltered conditions: Impact of Reynolds number and wind direction," *J. Wind Eng. Ind. Aerodyn.*, vol. 207, no. September, 2020.

[15] V. Kulkarni, N. Sahoo, and S. D. Chavan, "Simulation of honeycomb-screen combinations for turbulence management in a subsonic wind tunnel," *J. Wind Eng. Ind. Aerodyn.*, vol. 99, no. 1, pp. 37–45, 2011.

[16] Y. Seo, "Effect of hydraulic diameter of flow straighteners on turbulence intensity in square wind tunnel," *HVAC R Res.*, vol. 19, no. 2, pp. 141–147, 2013.

[17] J. L. Song, J. W. Li, and R. G. J. Flay, "Field measurements and wind tunnel investigation of wind characteristics at a bridge site in a Y-shaped valley," *J. Wind Eng. Ind. Aerodyn.*, vol. 202, no. November 2019, p. 104199, 2020.

[18] M. K. Panda and A. K. Samanta, "Design of low cost open circuit wind tunnel - A case study," *Indian J. Sci. Technol.*, vol. 9, no. 30, pp. 1–7, 2016.

[19] Ismail *et al.*, "Computational fluid dynamics simulation of the turbulence models in the tested section on wind tunnel," *Ain Shams Eng. J.*, vol. 11, no. 4, pp. 1201–1209,, 2020.

[20] Ismail, J. John, W. Libyawati, D. Rhakasywi, and A. Suwandi, "Optimization Design of

Open Circuit Wind Tunnel Suction Type," *Int. J. Mech. Mechatronics Eng.*, vol. 17, no. 06, p. 121, 2017.

[21] B. Yang, B. Zhang, X. Zhou, Y. Ren, and Y. Zhang, "Artificial simulation of complex unsteady wind in an ABL wind tunnel with dual axial fans," *J. Wind Eng. Ind. Aerodyn.*, vol. 197, no. August 2019, p. 104075, 2020.

[22] N. Su, S. Peng, N. Hong, and T. Hu, "Wind tunnel investigation on the wind load of large-span coal sheds with porous gables: Influence of gable ventilation," *J. Wind Eng. Ind. Aerodyn.*, vol. 204, no. July, p. 104242, 2020.

[23] B. Celis and H. H. Ubbens, "Design and Construction of an Open-circuit Wind Tunnel with Specific Measurement Equipment for Cycling," in *Procedia Engineering*, 2016, vol. 147, pp. 98–103.

[24] D. Damljanovic, J. Isakovic, and M. Milos, "Wind tunnel measurement quality in testing of a standard model," *Mater. Today Proc.*, vol. 4, no. 5, pp. 5791–5796, 2017.

[25] The Dutch Road Authority, "Measuring protocol wind," 2013.

[26] K. Ghorbanian, M. R. Soltani, and M. D. Manshadi, "Experimental investigation on turbulence intensity reduction in subsonic wind tunnels," *Aerosp. Sci. Technol.*, vol. 15, no. 2, pp. 137–147, 2011.

Contribution of individual authors to the creation of a scientific article (ghostwriting policy)

Ismail: Conceptualization and Methodology.
Johanis John: Formal analysis.
Erlanda Augupta Pane: Software.
Rahman Maulana: Investigation.
Reza Abdu Rahman: Writing – Review & Editing.
Agri Suwandi: Writing – Original Draft.

Sources of funding for research presented in a scientific article or scientific article itself

The authors were grateful to The Ministry of Research, Technology, and Higher Education of the Republic of Indonesia as being the funder of research that registered in letter No.3/E/KPT/2018.

Creative Commons Attribution License 4.0 (Attribution 4.0 International , CC BY 4.0)